Chapter 12
Changing Biogeochemistry in the South China Sea

Chen-Tung Arthur Chen, Shujie Yu, Ting-Hsuan Huang, Hon-Kit Lui, Yan Bai, and Xianqiang He

Abstract The tropical/subtropical South China Sea (SCS) is the largest marginal sea in the world. Like other warm bodies of water, its sea surface temperature (SST) is rising, albeit more slowly (0.012 °C/yr between 1998 and 2016) than that of cold-water regions at high latitudes. The chlorophyll concentration increased at 0.0012 μg/L/yr during that period, and the Secchi disk depth (SDD) increased by 0.035 m/yr. The changes of SST, chlorophyll concentration and SDD, the factors governing changes in ocean biogeochemistry, in the SCS exhibit high temporal-spatial variability, and these parameters varied in opposite directions during the periods 1998–2008 and 2008–2016. The first period witnessed declining SST and SDD and increasing chlorophyll concentration, referring to enhancing primary productivity. The second period witnessed increasing SST and SDD but falling chlorophyll concentration, referring to declining primary productivity. These changes and increasing anthropogenic activities on land may be related to changing biogeochemistry such as decreasing dissolved oxygen concentration in coastal regions. In the SCS basin, however, particulate organic carbon and nitrogen seem to be on the rise.

C.-T. A. Chen (✉) · T.-H. Huang · H.-K. Lui
Department of Oceanography, National Sun Yat-Sen University, Kaohsiung 804, Taiwan
e-mail: ctchen@mail.nsysu.edu.tw

T.-H. Huang
e-mail: thhuang@mail.nsysu.edu.tw

H.-K. Lui
e-mail: hklui@mail.nsysu.edu.tw

S. Yu · Y. Bai · X. He
State Key Laboratory of Satellite Ocean Environment Dynamics, Second Institute of Oceanography, Ministry of Natural Resources, Hangzhou 310012, China
e-mail: yvshujie@126.com

Y. Bai
e-mail: baiyan@sio.org.cn

X. He
e-mail: hexianqiang@sio.org.cn

C.-T. A. Chen and X. Guo (eds.), *Changing Asia-Pacific Marginal Seas*, Atmosphere, Earth, Ocean & Space, https://doi.org/10.1007/978-981-15-4886-4_12

Keywords South China Sea · Sea surface temperature · Salinity · Chlorophyll · Secchi disk depth · pH · Temporal changes

12.1 Introduction

The South China Sea (SCS), with an area of 3.5×10^6 km^2, is the largest marginal sea in the world (Fig. 12.1). Like the oceans, it is undergoing the consequences of the global environmental change. Although the SCS encompasses a large area and an average depth of about 1350 m, it is actually semi-enclosed because the Sunda Shelf and the Gulf of Thailand in its southern and southwestern regions are rather shallow, with an average depth of only 50 m. The wide Sunda Shelf connects to the Indian Ocean via the Strait of Malacca to the southwest, but the major connection is with the Java Sea to the southeast through the Karimata and Gelasa Straits which are less than 50 m deep. The northern and northwestern regions of the SCS are also wide shelves that connect to the East China Sea (ECS) via the shallow Taiwan Strait, which has an average depth of only 50 m (Fig. 12.1).

The central and northeastern parts of the SCS are as deep as 5500 m but the only deep linkages to areas beyond the sea are the 400 m-deep Mindoro Strait, which connects to the Sulu Sea, and the 2200 m-deep Luzon Strait, which opens into the West Philippine Sea (WPS). Since the ridge that separates the Sulu Sea from the water beyond it is only approximately 100 m deep, water that is deeper than about 100 m in the Pacific Ocean can only enter the SCS through the Luzon Strait. Monsoon

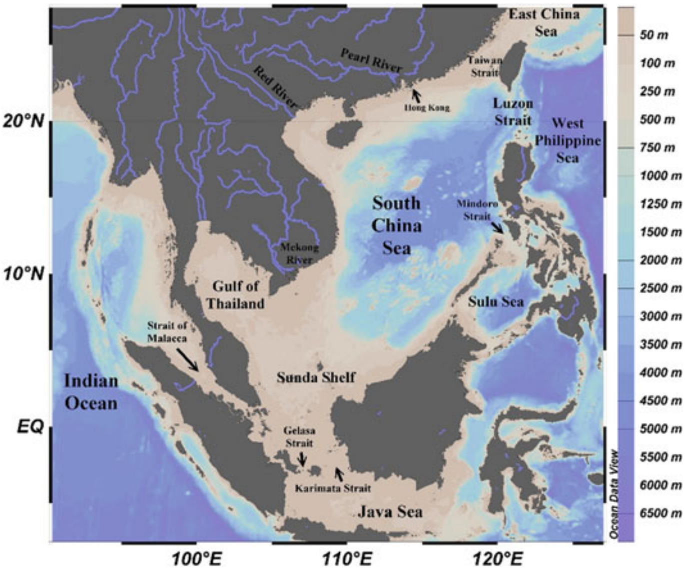

Fig. 12.1 Map of the South China Sea

winds dominate the circulation in the SCS and exchanges of seawater with the water outside it (Chao et al. 1996a, b; Qu 2000; Wu and Chang 2005). Since no deep or intermediate water forms in the SCS because cooling in winter is too little to make the water very dense, unique subsurface features, such as extreme salinity are brought in from the WPS. Subsequent vertical mixing and upwelling diminish these features (Chen and Huang 1996).

The anthropogenic release of CO_2 undoubtedly caused the problem of so-called global environmental change. The oceans are a major sink of excess anthropogenic CO_2, some of which has penetrated to the bottom of the oceans (Chen and Millero 1979; Chen and Pytkowicz 1979; Chen 2003; Chen et al. 2006a, b). Like the global oceans, the SCS has experienced a fall in pH as a result of the increase in the concentration of CO_2 in the atmosphere (Chai et al. 2009; Liu et al. 2014; Lui and Chen 2015). Perhaps owing to the upwelling, however, anthropogenic CO_2 penetrates to a depth of only roughly 1500 m in the SCS (Chen et al. 2006a, b) although signals near the detection limit have also been reported below 1500 m (Huang et al. 2016). As the saturation horizon of calcite exceeds a depth of 2000 m in the SCS (Chen and Huang 1995), excess CO_2 penetration is expected to enhance its dissolution only slightly. The saturation horizon of aragonite, however, is only 600 m, which is less than the depth of excess CO_2 penetration but greater than the aragonite saturation horizon in the Bering Sea (Chen et al. 2020a). As a result, an upward migration of the saturation horizon affects the aragonite deposits on the SCS shelf, but less than it affects the deposits in the Bering Sea.

The salinity of the SCS surface water has reportedly been declining during the last two decades (Fig. 12.2; Nan et al. 2016), consistent with the general trend that relatively fresh seas, including several marginal seas, are experiencing falling salinity while more saline regions, such as the North Pacific Subtropical Water have been increasing in salinity (Durack and Wijffels 2010). Interestingly, the freshening of the upper waters of the SCS is not caused by increasing river discharge, because all three major rivers that enter the SCS—the Mekong, Pearl and Red Rivers—experienced a declining outflow between 1993 and 2012 (Nan et al. 2016). Precipitation increased

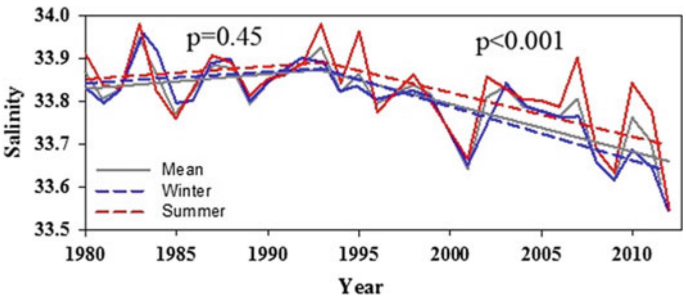

Fig. 12.2 Time series of salinity in the winter (Dec.–Feb.; blue), the summer (Jun.–Aug.; red), and mean (black) averaged above 100 m in the SCS. Dotted lines represent the linear trends before/after 1993 that best fit the data (modified from Nan et al. 2016)

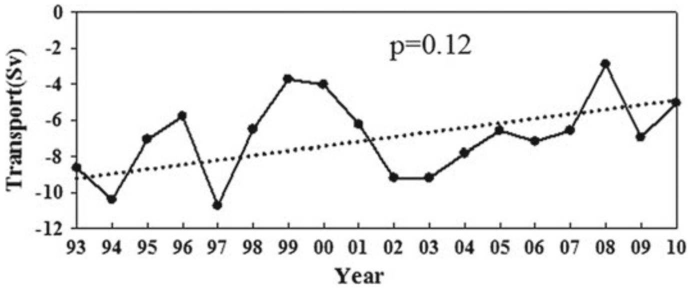

Fig. 12.3 Annual time series and linear trend of flux of Luzon Strait based on ROMS. Data taken from Nan et al. 2015 (Negative values represent westward flow)

to exceed evaporation during that period but the increase was responsible for only 15% of the seawater freshening (Nan et al. 2016). The major cause of 85% of the freshening was reportedly a decrease in the intrusion of salty Kuroshio water in those years (Nan et al. 2013, 2015; Fig. 12.3). Lui et al. (2018), however, reported an increase in Kuroshio intrusion in the Luzon Strait transport since 2012. Since the nutrient inventories in the euphotic layer of the WPS are significantly lower than that in the SCS, the intrusion of the WPS seawater decreases the nutrient inventories of the euphotic layer, and hence reduces primary production and export production in the SCS. These complicated processes influence the biogeochemistry of the SCS, but the impact of such factors as the El Nino-Southern Oscillation (ENSO) and the Pacific Decadal Oscillation (PDO) is unknown. For example, Fig. 12.4 plots a time series of anomalies of alkalinity, dissolved inorganic carbon, nitrogen, phosphorus and silicate concentrations as well as water transport from the SCS to the ECS. Overall, they tend to rise, and this trend is clearly related to anomalous change in sea surface height (Fig. 12.4h). These signals correlate with PDO (Fig. 12.4j). Recent changes in SST, chlorophyll, Secchi disk depth (SDD) and related carbonate chemistry will be discussed below.

12.2 Changing Sea Surface Temperature

The SST data for the period from 1998 to 2016 were taken from the AVHRR_OI dataset, which is a product of the Group for High-Resolution Sea Surface Temperature (GHRSST), and can be obtained from the National Center for Environmental Information (NCEI), NOAA (https://data.nodc.noaa.gov/ghrsst/L4/GLOB/NCEI/AVHRR_OI/ghrsst/L4/GLOB/NCEI/AVHRR_OI/). Data were averaged monthly from 1998 to 2016. Details can be found in Chen et al. (2020a).

Figure 12.5a displays a climatological map of the SST, which typically exceeds 26 °C except in the coastal region southeast of China, mainly because the cold Chinese coastal water flows southward from September to May when the NE monsoon

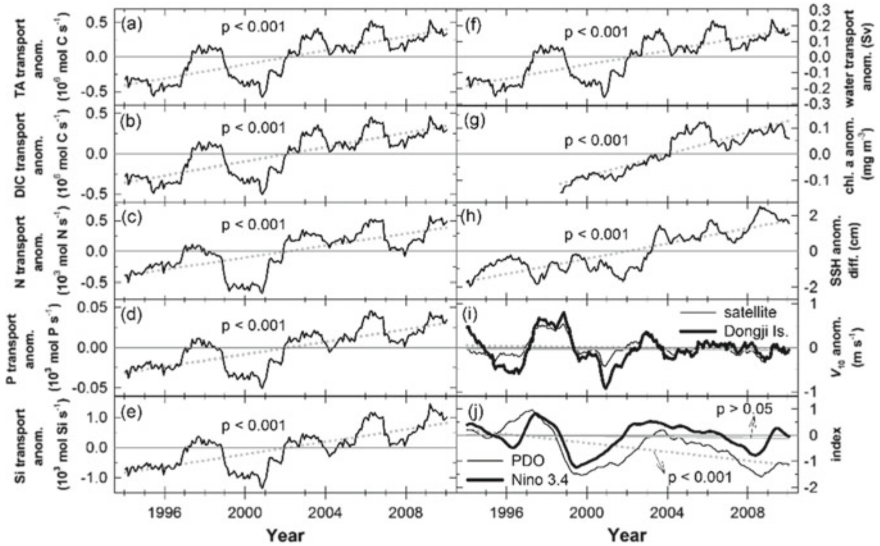

Fig. 12.4 Twenty-four month moving average time series of anomalies and their regression lines in the Taiwan Strait for **a** TA flux, **b** DIC flux, **c** N flux, **d** P flux, **e** Si flux, **f** water flux, **g** satellite chl. a concentration, **h** difference in SSH between southern and northern entrances, **i** wind speed measured by the satellite and at the weather station in the south-north direction at a height of 10 m, and **j** PDO and Niño 3.4 indices. Dashed and solid lines in (**i**) are regression lines from satellite data and weather station data, respectively. Dashed and solid lines in (**j**) are regression lines of PDO and Niño 3.4, respectively (taken from Huang et al. 2019)

prevails. This cold water brings nutrients from the ECS to the SCS (Chen 2003; Naik and Chen 2008; Han et al. 2013).

Figure 12.6a plots the temporal variation of the SST. Unlike in high-latitude seas, where the SST exhibits a large seasonal variation (Chen et al. 2020a, b), in the SCS, the mean SST varies only between about 25 and 30 °C. Also, whereas the temperature from 1998 to 2016 in the high-latitude seas generally increased (0.055 °C/yr for the Bering Sea (Chen et al. 2020a); 0.045 °C/yr for the Okhotsk Sea (Chen et al. 2020b)), that in the SCS exhibited only a statistically insignificant linear increase of 0.12 °C/yr ($p = 0.46$). The quadratic polynomial fit of the SST has a lower p value of 0.14 (better correlation) than the linear fit (Fig. 12.6a). The quadratic fit seems to indicate that the SST initially fell after the strong El Nino year of 1998 when basin-wide warming occurred in the SCS (Wu and Chang 2005), and increased in subsequent years. The mixed layer, however, seems to have become shallower from 1992 to 2000 (Li et al. 2017) consistent with a rise in SST, especially during the strong El Nino years of 1997 and 1998.

Many reports of interannual SST variations in the SCS have been published, but the results vary with the time span considered. He et al. (2017) reported little change in the SST between 1998 and 2010. Giuliani et al. (2019) reported an increase of 0.028 ºC/yr from 1960 to 2011, which is close to that obtained by Bai et al. (2018)

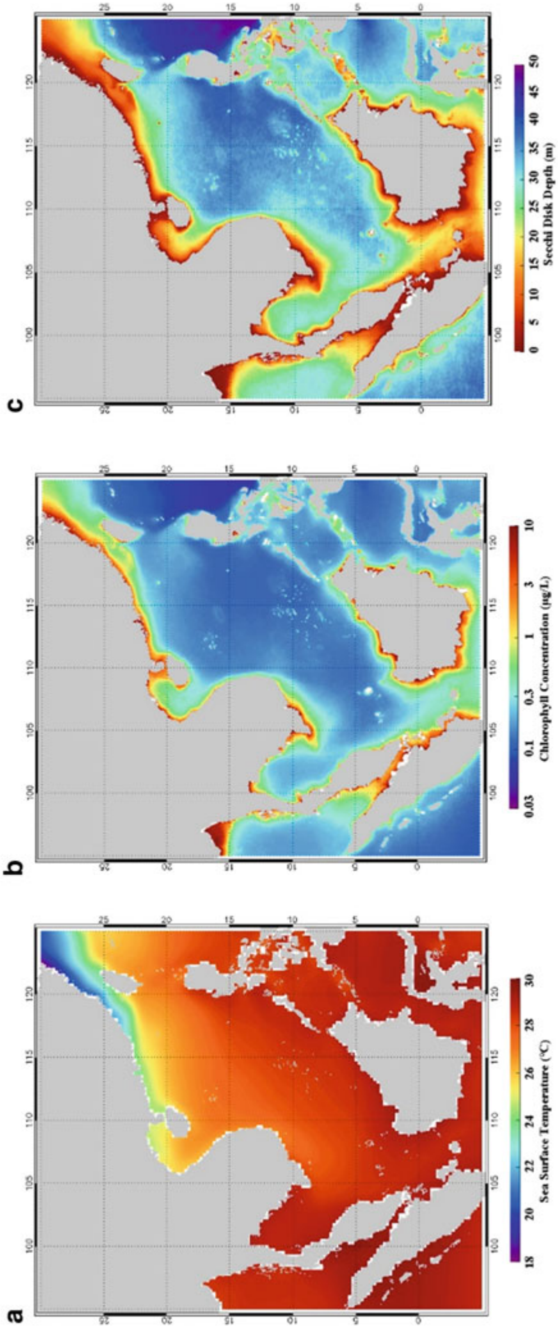

Fig. 12.5 Climatological map of **a** SST, **b** chlorophyll concentration and **c** SDD in the South China Sea

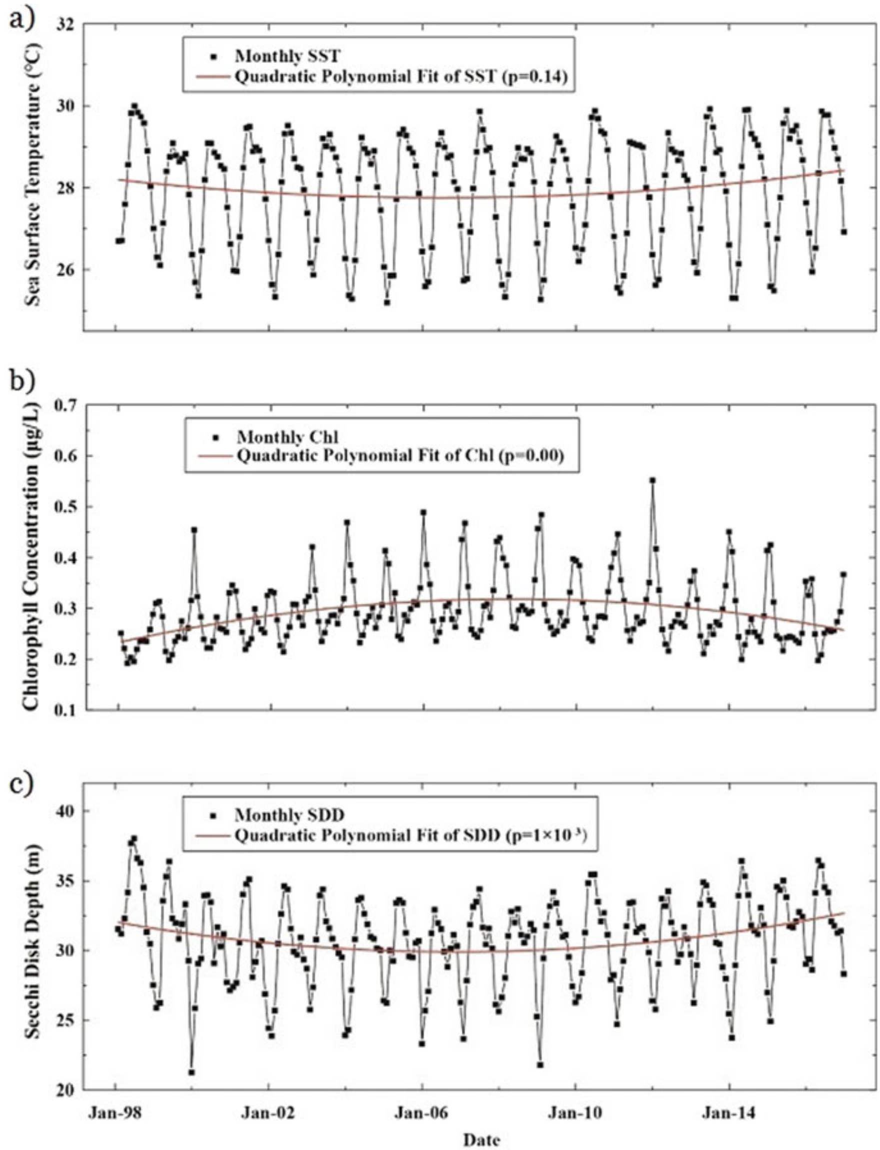

Fig. 12.6 Time series of **a** SST, **b** chlorophyll concentration and **c** SDD in the SCS during 1998–2016

(around 0.03 °C or 0.1%/yr from 2003 to 2014) in low-latitude marginal seas around the Eurasian continent, including the SCS, the Java-Banda Sea, the Bay of Bengal and the Arabian Sea. Chapter 1 noted that higher-latitude marginal seas exhibited larger temperature increases.

Geographically, the region off SE China where the average SST is the lowest of any part of the SCS saw a decrease in the SST, while the warmest regions in the southern SCS saw an increase in the SST. Figure 12.7a demonstrates that the SST in the mid- and southern SCS increased at a significant rate of 0.01–0.02 °C per year over the period 1998–2016. Notably, the SST fell remarkably both off SE China and in the Taiwan Strait, where the chlorophyll concentration significantly increased (Fig. 12.7b). The cooling may suggest strengthening of coastal upwelling, which would have resulted in an increase of surface nutrient supply, favoring the growth of phytoplankton.

12.3 Changing Chlorophyll Concentration

The chlorophyll concentration data for the period 1998–2016 were obtained from the Ocean Colour project of the ESA Climate Change Initiative (CCI) (http://www.esa-oceancolour-cci.org). Details can be found in Chen et al. (2020a).

As expected, because of riverine input of nutrients, entrainment by river plumes, coastal upwelling, and more effective wind and tidal mixing, the coastal regions in the SCS had higher chlorophyll concentrations than more open, deeper waters (Fig. 12.5b; Chen 2008; Chen et al. 2020a, b). In 1998–2016, chlorophyll concentrations rose significantly on the northern shelf of the SCS and off the Indochina Peninsula (Fig. 12.7b). In the Taiwan Strait and in the northern SCS, the chlorophyll concentration generally increased at the rate of 2.5% per year (Fig. 12.7b). Increased anthropogenic nutrient inputs might have contributed to the increase in chlorophyll concentration in these coastal waters. Patches of decreasing chlorophyll concentration formed sporadically in the central basin of the SCS, in which the chlorophyll concentration fell at 1–1.5% per year. Overall, the whole SCS exhibited a very small average annual increase of 0.0012 μg/L ($p = 0.11$) from 1998 to 2016 (Fig. 12.6b). The quadratic polynomial fitting indicates that chlorophyll concentration in the SCS firstly rose and then fell. Figure 12.6b shows an increase from Jan. 1998 to Apr. 2008 and a decrease from Apr. 2008 to Dec. 2016. In contrast, from 1998 to 2016, the chlorophyll concentration increased steadily in the Bering Sea (0.011 μg/L/yr, Chen et al. 2020a) and the Okhotsk Sea (0.01 μg/L/yr, Chen et al. 2020b).

He et al. (2017) reported no apparent change in chlorophyll concentration in the SCS between 1997 and 2010, whereas Palacz et al. (2011) reported an increase of 0.04 μg/L (9%) over that period. The data that were generated by modeling of Li et al. (2015) indicate an increase between 2000 and 2014 although the lead author of that paper, Q. P. Li (personal communication, 12/1/2018) identified no clear trend. They also did not consider lateral transports. Bai et al. (2018), reported a very small rate of increase of <0.001 μg/L per year between 2003 and 2014, in contrast to

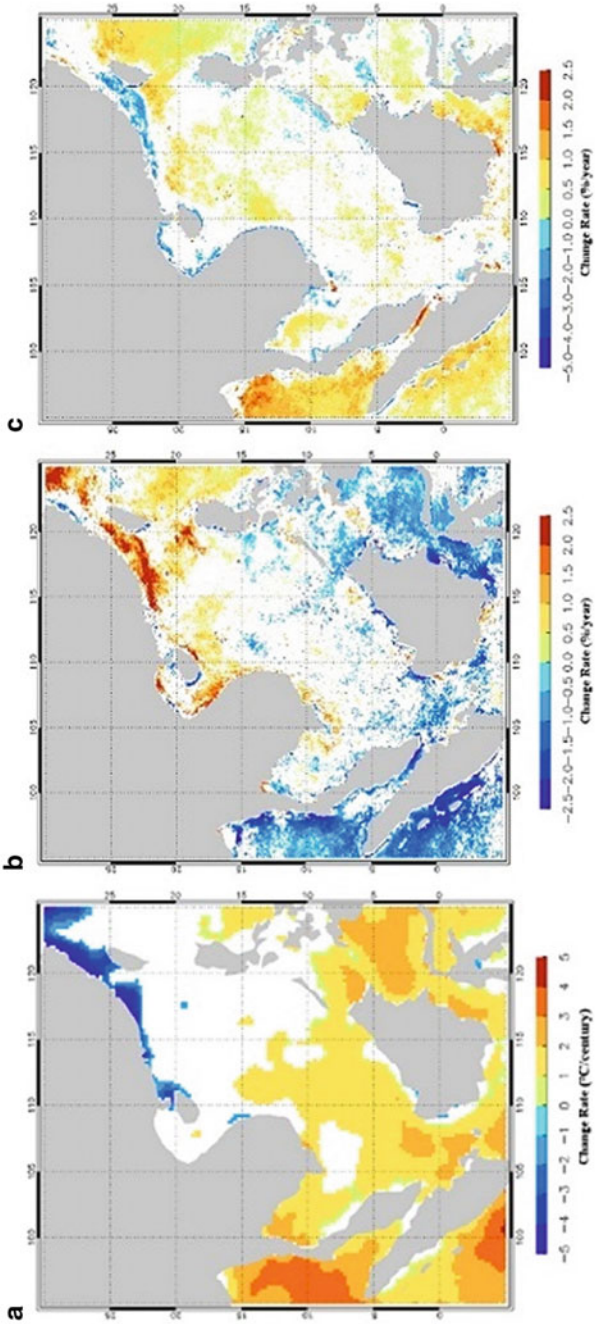

Fig. 12.7 Temporal variations of **a** SST, **b** chlorophyll concentration and **c** SDD in the SCS during 1998–2016 (Only pixels that are associated with significance at $P < 0.1$ are shown in bright colors)

decreases in other tropical marginal seas, such as the Arabian Sea, the Java-Banda Sea, the Red Sea, the Persian Gulf and the Bay of Bengal. In fact, a close look at the interannual variability of chlorophyll concentration in the SCS (Fig. 12.6b) suggests that the concentration increased between 1998 and 2008 but decreased thereafter. As mentioned earlier, 1998 was a strong El Nino year in which the SST was high. The high SST resulted in relatively low-density surface water and a relatively high density gradient. Therefore vertical mixing was less than in other years, so fewer nutrients were pumped to the surface layer, resulting in lower primary productivity, chlorophyll, diatom biomass and biological productivity in general (Lu et al. 2018). Future changes are, however, difficult to predict as a higher SST would impede the upward transport of nutrients whereas riverine input is rising. The physiological responses of many marine organisms, to variables other than nutrient availability, such as those caused by typhoons, eddies, atmospheric deposition and nitrogen fixation, may also change (Li et al. 2015; Wu and Chang 2005; Wong et al. 2002). Notably, oxygen inventories have been increasing in the SCS contrary to most other oceans (Schmidtko et al. 2017; Breitburg et al. 2018). The oxygen inventory increased perhaps because of the decreasing SST (higher oxygen solubility) and enhanced productivity, as revealed by the increasing chlorophyll concentration there. Ito et al. (2017) also reported increasing oxygen concentration between 100 and 700 m.

Interestingly, the collection of particles in sediment traps at 2,000 m and 3,500 m depths in the basin of the SCS indicates that proportions of the particulate organic carbon (POC) and particulate organic nitrogen (PON) increased with time but the POC/PON ratio decreased (Fig. 12.9) probably because of increasing anthropogenic nutrient outflows with the consequence that the chlorophyll concentration off Hong Kong has been increasing since 1990 (Fig. 12.8a). The dissolved oxygen concentration in the bottom layer, however, seems to be falling (Fig. 12.8b), perhaps due to an increase in the decomposition of phytoplankton from 2008 to 2016 (Fig. 12.8; Lui et al. 2018). Intuitively, this finding seems to be inconsistent with the fall in chlorophyll concentration that was observed during the same period. The result is interesting because in the basin of the SCS, lower the net primary productivity corresponds to higher export efficiency (Li et al. 2018). In the SCS, primary productivity correlates positively with chlorophyll concentration (Chen 2005) so the decreasing chlorophyll concentration between 2008 and 2016 reflects a fall in net primary productivity. As a result, the export efficiency increased, resulting in higher proportions of POC and PON in the sediment traps. The increases in the POC and PON percentages are probably not caused by an increase in riverine outflow. A larger amount of terrestrial organic matter would have corresponded to a higher POC/PON ratio but this was not observed (Fig. 12.9c). Notably, the increasing POC percentage that was reported by Lui et al. (2018) covered only a relatively short period from 2008 to 2016. The POC flux (Li et al. 2017) actually seems to have decreased between 1992 and 1999. Multi-decadal data are required to identify any genuine long-term trend.

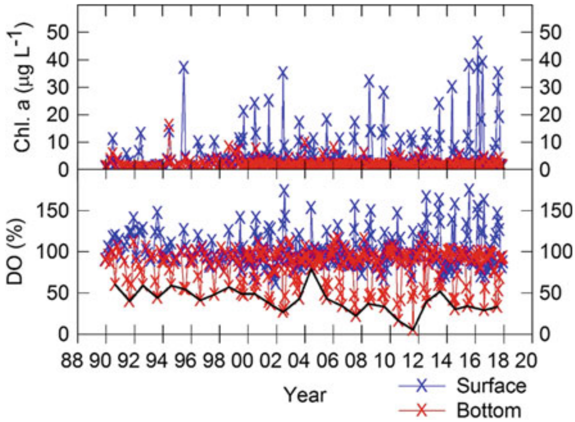

Fig. 12.8 Time series of **a** chlorophyll concentration and **b** dissolved oxygen off Hong Kong (taken from Lui et al. 2020)

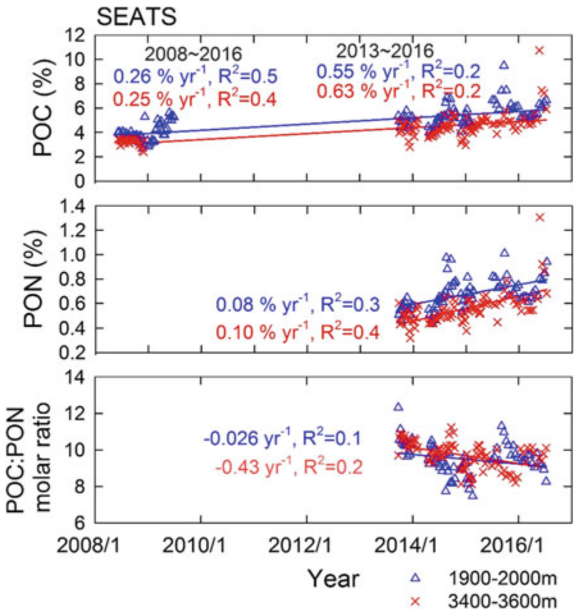

Fig. 12.9 Percentages of **a** POC and **b** PON in sinking particles, and the **c** POC:PON molar ratio at various depths at SEATS between 2008 and 2016. The POC data between 2008/6/10 and 2009/6/30 were taken from Wei et al. 2017. Solid lines and numbers are regression lines, slopes, and coefficient of determination. All regression lines have $p < 0.0001$, apart from that for POC:PON ratio at 2000 m for which $p = 0.04$ (taken from Lui et al. 2018)

12.4 Changing Secchi Disk Depth

The SDD is a good index of water transparency, and pertinent data for the period 1998–2016 were provided by the Globcolour project (http://globcolour.info/). Details can be found in Chen et al. (2020a). Figure 12.5c displays the distribution of the SDD. As expected, the SDD is shallow close to the coast because of the relatively high phytoplankton biomass there, as indicated by the high chlorophyll concentration (Fig. 12.5b), and the large amount of suspended sediment due to river transport.

Mixing by winds and tides in shallow waters also reduces the SDD, which throughout almost the entire SCS increased during the period 1998–2016 (0.35 m/yr, p = 0.35, Fig. 12.7c), showing that the SCS water became more transparent. The fitting revealed that the SDD in the SCS decreased from Jan. 1998 to Nov. 2008 and then increased from Nov. 2008 to Dec. 2016 (Fig. 12.6c). However, the SDD in coastal waters substantially decreased (Fig. 12.7c), especially off the coast of SE China and in the Taiwan Strait, perhaps because of the increase in chlorophyll concentration (Fig. 12.7b).

He et al. (2017) reported a decrease in the SDD in the SCS of about 0.08 m/yr from 1998 to 2010. A close look at the temporal change of the SDD from 1998 to 2016 (Fig. 12.6c) indicates that it decreased from 1998 to about 2008, consistent with the findings of He et al. (2017). The SDD increased after 2008. Bai et al. (2018) recently found that the SDD in all 12 marginal seas around the Eurasian continent increased from 2003 to 2014. They reported a rate of increase of 0.05 m/yr, which is slightly higher than the value obtained herein, which is 0.035 m/yr. The difference between the rates of increasing may be a result of a difference in the study periods. Chen et al. (2020a) reported no significant change in the SDD in the Bering Sea, and Chen et al. (2020b) reported a slight increase in the SDD (0.018 m/yr) in the Okhotsk Sea.

12.5 Conclusions

From 1998 to 2016, the SST in the SCS increased by 0.012 °C/yr, which is much less than the rate of warming of high-latitude oceans. This result is consistent with the generally declining salinity of the surface water of the SCS. The chlorophyll concentration increased at an overall rate of 0.0012 μg/L/yr. The significant increase in chlorophyll concentration occurred mainly on the northern shelf of the SCS and off the Indochina Peninsula. The SDD throughout the SCS increased by 0.035 m/yr in the same period. However, the SST, chlorophyll concentration and SDD in the SCS changed in opposite directions in the two periods 1998–2008 and 2008–2016. In the first period, the SST and SDD decreased while the chlorophyll concentration increased. In the second period, the SST and SDD increased but the chlorophyll concentration decreased. Since in the SCS basin, a lower net primary productivity corresponded to higher export productivity, reduced chlorophyll concentration yielded higher observed percentages of POC and PON that collected in sediment traps. All such changes might have altered the biogeochemical processes in the SCS.

Acknowledgements Preparation of this chapter was supported by the Ministry of Science and Technology (MOST 107-2611-M-110-006 and 107-2611-M-110-021) and the Ministry of Education (Higher Education Sprout Program) of Republic of China. Two anonymous reviewers provided valuable comments which strengthened the manuscript.

References

Bai Y, He XQ, Yu SJ, Chen CTA (2018) Changes in the ecological environment of the marginal seas along the Eurasian Continent from 2003 to 2014. Sustainability 10(3):635. https://dx.doi.org/10.3390/su10030635

Breitburg D, Levin LA, Oschlies A, Gregoire M, Chavez FP, Conley DJ, Garcon V, Gilbert D, Gutierrez D, Isensee K, Jacinto GS, Limburg KE, Montes I, Naqvi SWA, Pitcher GC, Rabalais NN, Roman MR, Rose KA, Seibel BA, Telszewski M, Yasuhara M, Zhang J (2018) Declining oxygen in the global ocean and coastal waters. Science 359:46 (6371), eaam7240

Chai F, Liu GM, Xue HJ, Shi L, Chao Y, Tseng CM, Chou WC, Liu KK (2009) Seasonal and interannual variability of carbon cycle in South China Sea: a three-dimensional physical-biogeochemical modeling study. J Oceanogr 65(5):703–720

Chao SY, Shaw PT, Wu SY (1996a) El Nino modulation of the South China Sea circulation. Prog Oceanogr 38(1):51–93

Chao SY, Shaw PT, Wu SY (1996b) Deep water ventilation in the South China Sea. Deep-Sea Res Pt I 43(4):445–466

Chen CT, Millero FJ (1979) Gradual increase of oceanic CO_2. Nature 277(5693):205–206

Chen CT, Pytkowicz RM (1979) Total CO_2 titration alkalinity oxygen system in the Pacific ocean. Nature 281(5730):362–365

Chen CTA (2003) Rare northward flow in the Taiwan Strait in winter: a note. Cont Shelf Res 23(3–4):387–391

Chen CTA (2008) Buoyancy leads to high productivity of the Changjiang diluted water: a note. Acta Oceanol Sin 27(6):133–140

Chen CTA, Huang MH (1995) Carbonate chemistry and the anthropogenic CO_2 in the South China Sea. Acta Oceanolog Sin 14:47–57

Chen CTA, Huang MH (1996) A mid-depth front separating the South China Sea water and the West Philippine Sea water. J Oceanogr 52:17–25

Chen CTA, Hou WP, Gamo T, Wang SL (2006a) Carbonate-related parameters of subsurface waters in the West Philippine, South China and Sulu Seas. Mar Chem 99(1–4):151–161

Chen CTA, Wang SL, Chou WC, Sheu DD (2006b) Carbonate chemistry and projected future changes in pH and $CaCO_3$ saturation state of the South China Sea. Mar Chem 101(3–4):277–305

Chen CTA, SJ Yu, TH Huang, Y Bai, XQ He (2020a) Changes in temperature, chlorophyll concentration, and Secchi Disk Depth in the Bering Sea from 1998 to 2016. In: Chen CTA, Guo XY (eds) Changing Asia-Pacific marginal seas. Springer International Publishing (in press)

Chen CTA, SJ Yu, TH Huang, Y Bai, XQ He (2020b) Changes in temperature, chlorophyll concentration, and Secchi Disk Depth in the Okhotsk Sea from 1998 to 2016. In: Chen CTA, Guo XY (eds) Changing Asia-Pacific marginal seas. Springer International Publishing (in press)

Chen YLL (2005) Spatial and seasonal variations of nitrate-based new production and primary production in the South China Sea. Deep-Sea Res Pt I 52(2):319–340

Durack PJ, Wijffels SE (2010) Fifty-year trends in global ocean salinities and their relationship to broad-scale warming. J Climate 23(16):4342–4362

Giuliani S, LG. Bellucci, DH Nhon (2019) The coast of Vietnam: present status and future challenges for sustainable development. In: Sheppard C (ed) World seas: an environmental evaluation, 2nd edn, Chapter 19. Academic Press, pp 415–435

Han AQ, Dai MH, Gan JP, Kao SJ, Zhao XZ, Jan S, Li Q, Lin H, Chen CTA, Wang L, Hu JY, Wang LF, Gong F (2013) Inter-shelf nutrient transport from the East China Sea as a major nutrient source supporting winter primary production on the northeast South China Sea shelf. Biogeosciences 10(12):8159–8170

He XQ, Pan DL, Bai Y, Wang TY, Chen CTA, Zhu QK, Hao ZZ, Gong F (2017) Recent changes of global ocean transparency observed by SeaWiFS. Cont Shelf Res 143:159–166

Huang P, Zhang M, Cai M, Ke H, Deng H, Li W (2016) Ventilation time and anthropogenic CO_2 in the South China Sea based on CFC-11 measurements. Deep Sea Res Part I 116:187–199

Huang T-H, Chen C-TA, Lee J, Wu C-R, Wang Y-L, Bai Y, He X, Wang S-L, Kandasamy S, Lou J-Y, Tsuang B-J, Chen H-W, Tseng R-S, Yang YJ (2019) East China Sea increasingly gains limiting nutrient P from South China Sea. Sci Rep 9:5648. https://doi.org/10.1038/s41598-019-42020-4
Ito T, Minobe S, Long MC, Deutsch C (2017) Upper ocean O_2 trends: 1958–2015. Geophys Res Lett 44(9):4214–4223
Li QP, Wang YJ, Dong Y, Gan JP (2015) Modeling long-term change of planktonic ecosystems in the northern South China Sea and the upstream Kuroshio Current. J Geophys Res-Oceans 120(6):3913–3936
Li HL, Wiesner MG, Chen JF, Ling Z, Zhang JJ, Ran LH (2017) Long-term variation of mesopelagic biogenic flux in the central South China Sea: impact of monsoonal seasonality and mesoscale eddy. Deep-Sea Res Pt I 126:62–72
Li T, Bai Y, He XQ, Chen XY, Chen CTA, Tao BY, Pan DL, Zhang X (2018) The relationship between POC export efficiency and primary production: opposite on the Shelf and basin of the northern South China Sea. Sustainability 10(10): 3634. https://doi.org/10.3390/su10103634
Liu Y, Peng ZC, Zhou RJ, Song SH, Liu WG, You CF, Lin YP, Yu KF, Wu CC, Wei GJ, Xie LH, Burr GS, Shen CC (2014) Acceleration of modern acidification in the South China Sea driven by anthropogenic CO_2. Sci Rep 4:5148. https://doi.org/10.1038/srep05148
Lu W, Luo Y, Yan X, Jiang Y (2018) Modeling the contribution of the microbial carbon pump to carbon sequestration in the South China Sea. Sci China Earth Sci 11:1594–1604
Lui HK, Chen CTA (2015) Deducing acidification rates based on short-term time series. Sci Rep 5:11517. https://doi.org/10.1038/srep11517
Lui HK, Chen KY, Chen CTA, Wang BS, Lin HL, Ho SH, Tseng CJ, Yang Y, Chan JW (2018) Physical forcing-driven productivity and sediment flux to the deep basin of northern South China Sea: a decadal time series study. Sustainability 10(4): 971. https://doi.org/10.3390/su10040971
Lui HK, CTA Chen, WP Ho, SJ Yu, JW Chan, Y Bai, XQ He (2020) Transient carbonate chemistry in the expanded Kuroshio region, In: Chen CTA, Guo XY (eds) Changing Asia-Pacific marginal seas. Springer International Publishing (in press)
Naik H, Chen CTA (2008) Biogeochemical cycling in the Taiwan Strait. Estuar Coast Shelf S 78(4):603–612
Nan F, Xue HJ, Chai F, Wang DX, Yu F, Shi MC, Guo PF, Xiu P (2013) Weakening of the Kuroshio Intrusion into the South China Sea over the past two decades. J Climate 26(20):8097–8110
Nan F, Xue HJ, Yu F (2015) Kuroshio intrusion into the South China Sea: a review. Prog Oceanogr 137:314–333
Nan F, Yu F, Xue HJ, Zeng LL, Wang DX, Yang SL, Nguyen KC (2016) Freshening of the upper ocean in the South China Sea since the early 1990s. Deep-Sea Res Pt I 118:20–29
Palacz AP, Xue HJ, Armbrecht C, Zhang CY, Chai F (2011) Seasonal and inter-annual changes in the surface chlorophyll of the South China Sea. J Geophys Res-Oceans 116:C09015. https://doi.org/10.1029/2011jc007064
Qu TD (2000) Upper-layer circulation in the South China Sea. J Phys Oceanogr 30(6):1450–1460
Schmidtko S, Stramma L, Visbeck M (2017) Decline in global oceanic oxygen content during the past five decades. Nature 542(7641):335. https://doi.org/10.1038/nature21399
Wong GTF, SW Chung, FK Shiah, CC Chen, LS Wen, KK Liu (2002) Nitrate anomaly in the upper nutricline in the northern South China Sea-Evidence for nitrogen fixation. Geophys Res Lett 29(23):12-1–12-4
Wei CL, Chia CY, Chou WC, Lee WH (2017) Sinking fluxes of Pb-210 and Po-210 in the deep basin of the northern South China Sea. J Environ Radioactiv 174:45–53
Wu CR, Chang CWJ (2005) Interannual variability of the South China Sea in a data assimilation model. Geophys Res Lett 32:L17611. https://doi.org/10.1029/2005gl023798